Supplementary Information

Combined roles of ATP and small hairpin RNA in the activation of RIG-I revealed by solution-based analysis.

Neelam Shah[1], Simone A Beckham[1], Jacqueline A Wilce[1*] and Matthew CJ Wilce[1].

[1]Monash Biomedicine Discovery Institute and Department of Biochemistry and Molecular Biology, Monash University, Victoria 3800, Australia

Figure S1. Size exclusion chromatography profiles from SEC-SAXS of DC- and FL-RIG-I, apo and with 10bp or 8bp ± ATP analogues, AMP-PNP and ADP-AlF_x detected at 280 nm (solid black line) and 260 nm (dotted black line). Absorbances (in arbitrary units) are indicated on the Y axis and elution time (in min) indicated on the X-axis. Due to high background absorbance at 260 nm where ATP-analogues were included in the running buffer, the 260 nm were not useful and are thus not shown.

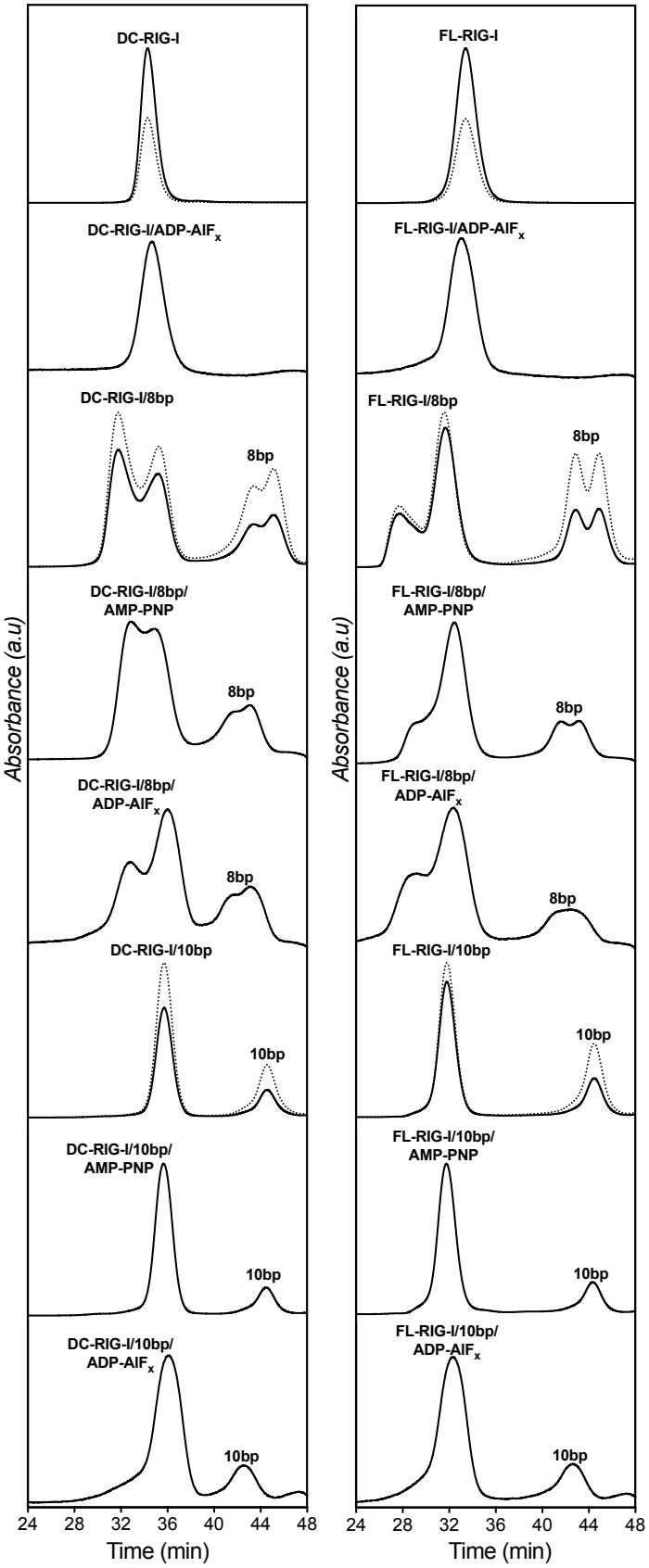

Figure S2. The Gaussian decomposition (represented by grey shading) of the baseline subtracted SAXS data (shown by black line) of DC- and FL-RIG-I, apo and with 10bp and 8bp ± ATP analogues shown in arbitrary units [I (a.u)] as a function of time (in min).

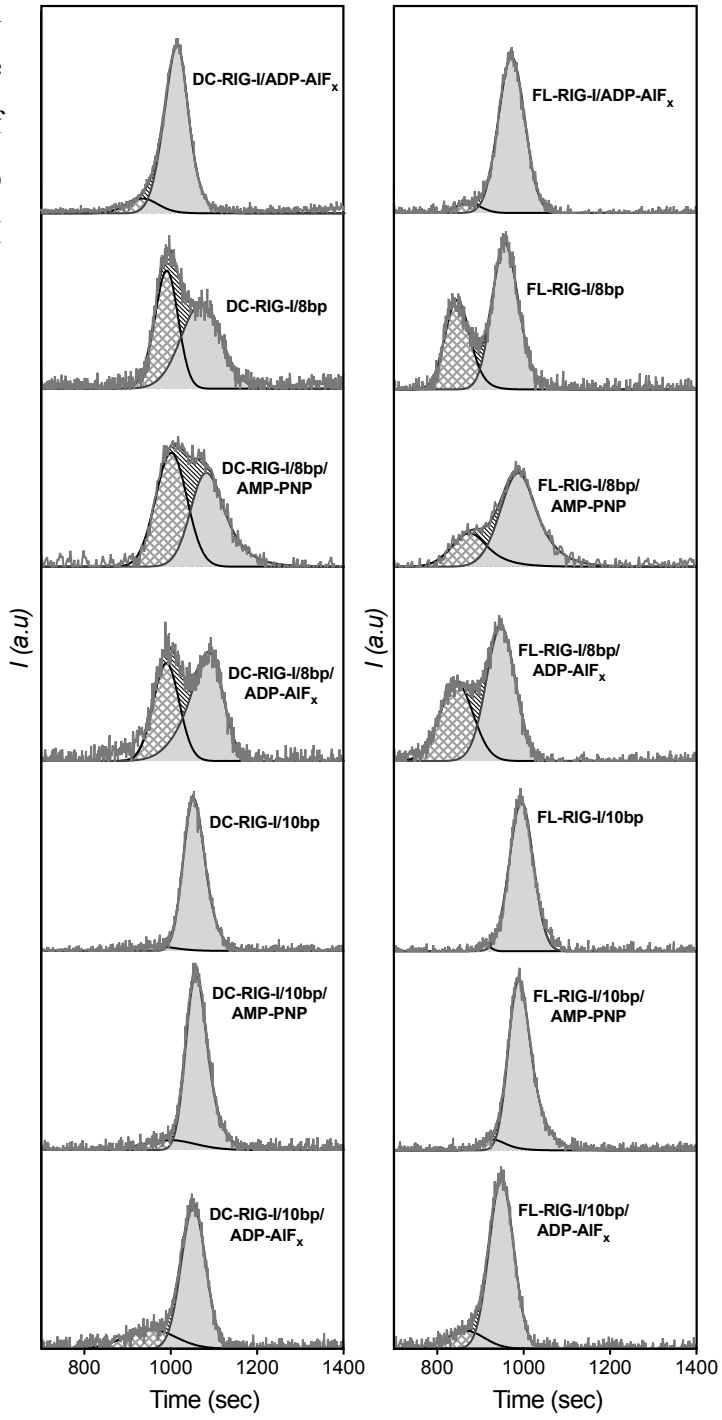

Figure S3. The predicted scattering curves from BUNCH and CORAL derived models (shown as grey lines) overlaid on experimental scattering profiles (shown as black spheres) of DC- and FL-RIG-I with no RNA (8bp or 10bp) or bound ATP analogue, and DC-RIG-I with 8bp or 10bp and ATP analogue. The scattering curves are shown with scattering intensity [log I(s)] as a function of forward scattering vector in the units of $Å^{-1}$.

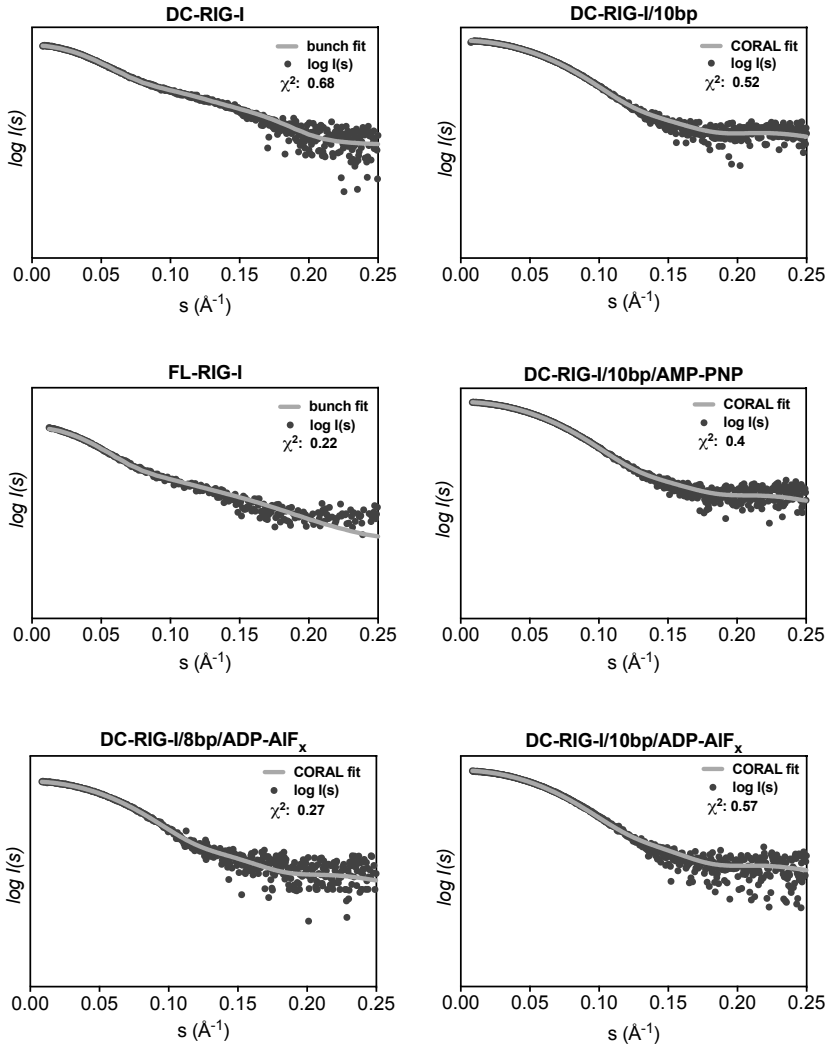

Figure S4A. The predicted scattering curves from EOM derived models (shown by grey lines) overlaid on experimental scattering profiles (shown by black spheres) of DC- and FL-RIG-I with and without RNA (8bp or 10bp) and ± ATP-analogue. These scattering curves are obtained by plotting log of scattering intensity [log I(s)] as a function of forward scattering vector in the units of $Å^{-1}$.

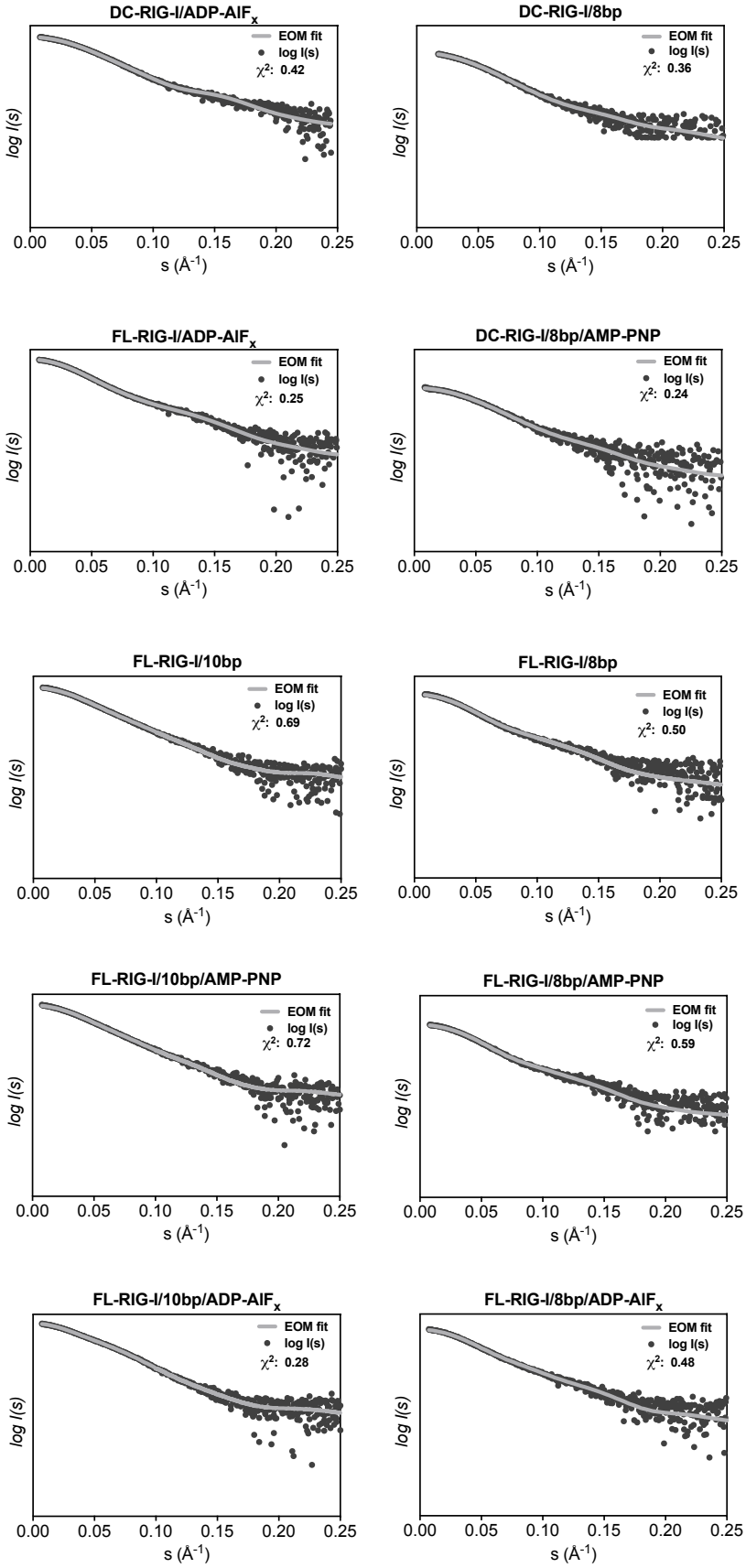

Figure S4B. An example of the individual predicted scattering curves derived from EOM models. TOP PANEL: shows the predicted scattering curve derived from combined EOM models of DC-RIG-I/ADP-AlF_x. BOTTOM PANEL: shows the individual predicted scattering curve derived from each of the three EOM models of DC-RIG-I/ADP-AlF_x. Predicted curves (shown by grey lines) are overlaid on the experimental scattering profile acquired for DC-RIG-I/ADP-AlF_x (shown by black spheres). These scattering curves are obtained by plotting log of scattering intensity [log I(s)] as a function of forward scattering vector in the units of $Å^{-1}$.

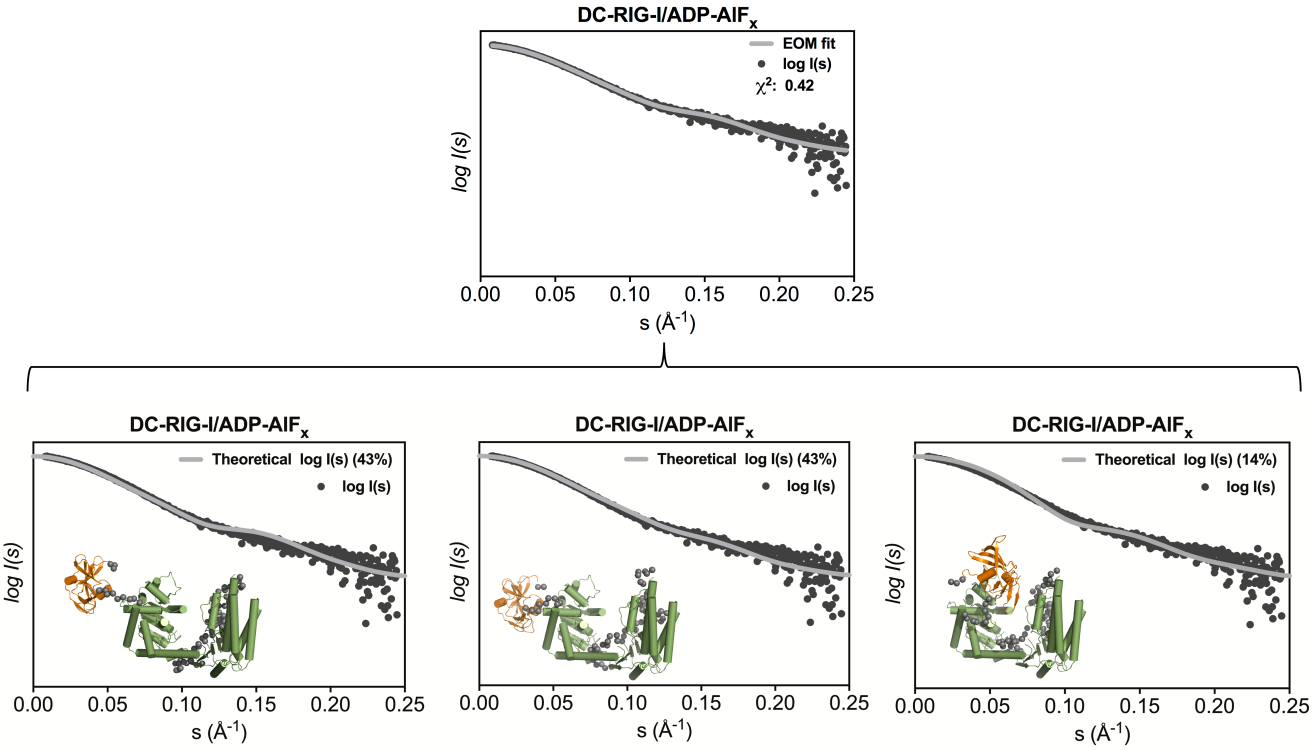

Figure S5. Assessment of purity and heterogeneity of 8bp hairpin dsRNA from SEC fractions of FL-RIG-I:8bp complex. Fractions across peaks 1 and 2 from SEC run of FL-RIG-I in complex with 5´ppp 8bp hairpin dsRNA (20mer) were run on denaturing **(A)** and native **(B)** polyacrylamide gel electrophoresis and visualized on Typhoon trio. Control RNA include: non-self annealing 29mer, self annealing 24mer and 10mer ssRNA). (**C)** shows the size exclusion chromatography profile of FL-RIG-I with 8bp-long in the absence of any ATP analogues detected at 280 nm (solid black line) and 260 nm (dotted black line). Absorbance (in arbitrary units [a.u]) is indicated on the Y axis and elution time (in min) indicated on the X-axis.

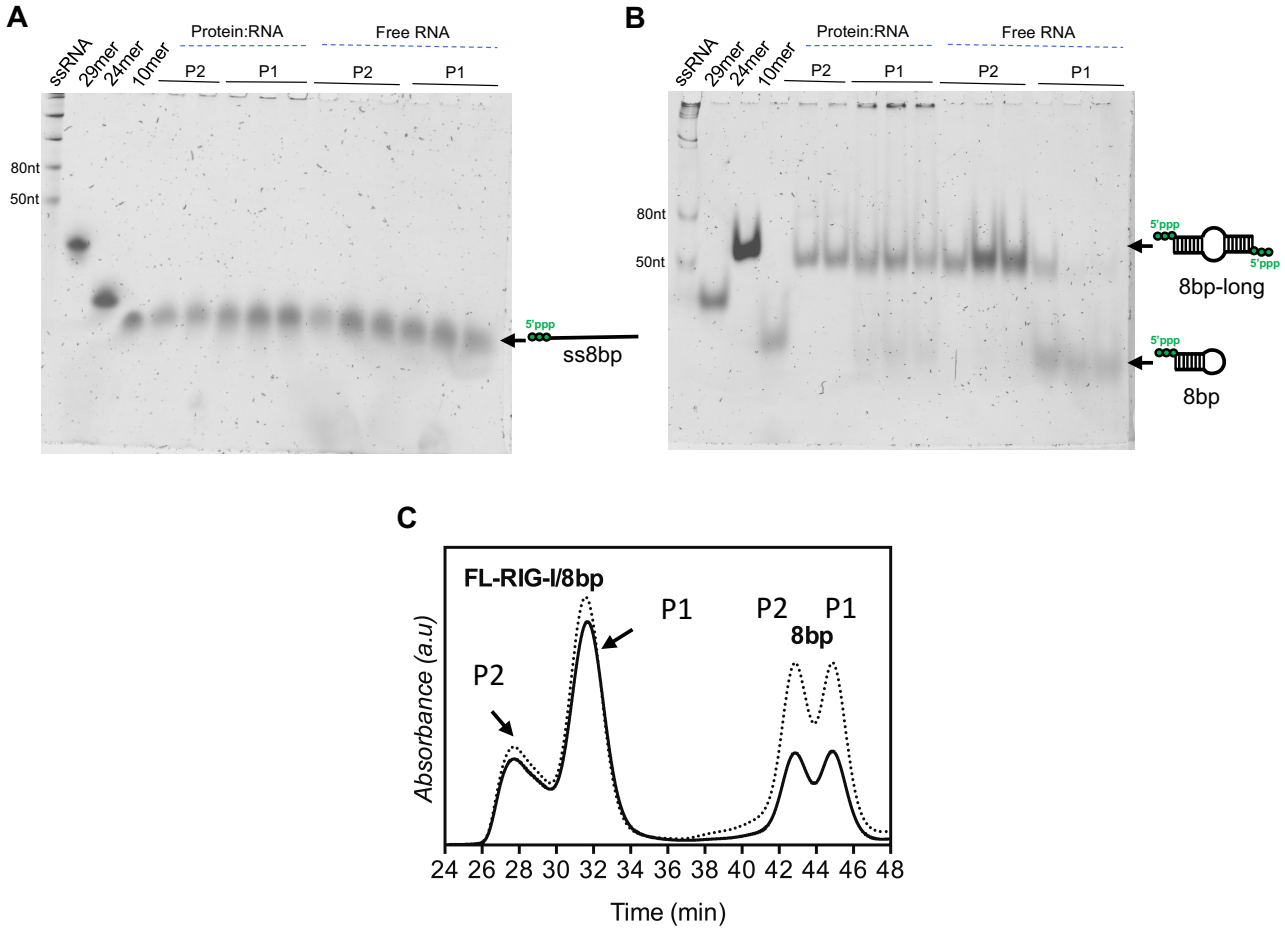

Figure S6. (A) Experimental scattering profiles of DC- and FL-RIG-I with 8b-long and their comparison with scattering profiles of 8bp complexes of RIG-I. Scattering profiles are shown as the scattering intensity [ln I(s)] as a function of forward scattering vector in the units of $Å^{-1}$ and represented by black spheres along with the grey error bars showing the mean ± SD, (**B)** pairwise distribution [P(r)] profiles of RIG-I with 8bp-long and their comparison with P(r) profiles of 8bp complexes obtained by plotting P(r) as a function of r in the units of Å.

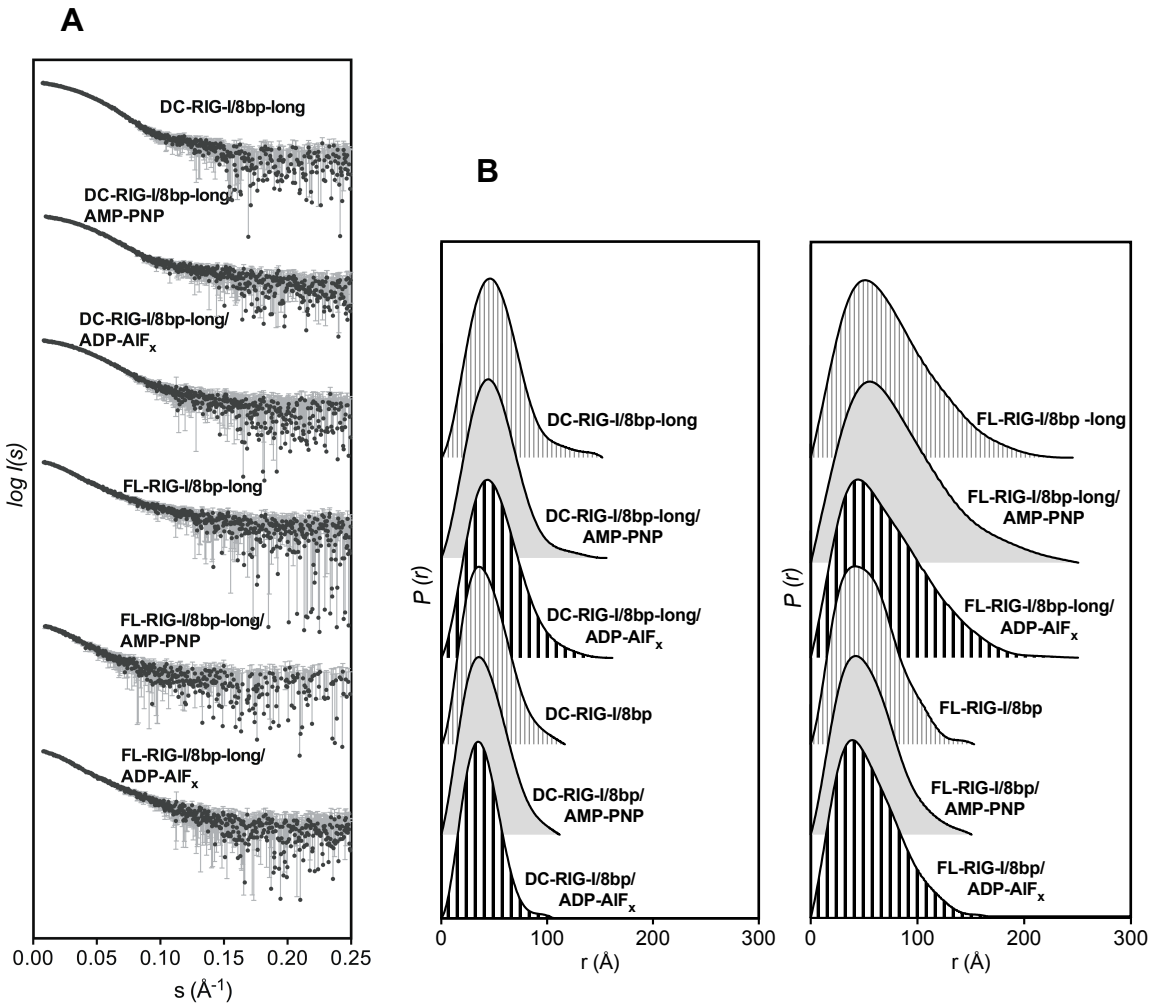

Figure S7. SAXS-derived model of DC-RIG-I molecules in complex with 8bp-long in the presence of ADP-AlF$_x$. **(A)** two phase MONSA (1) derived multiphase *ab initio* reconstruction of DC-RIG-I/10bp-long complex using SAXS data and represented as a molecular envelope with helicase and CTD domains shown in grey, and 8bp-long in blue. **(B)** SASREF (2) derived model of DC-RIG-I/8bp-long complex in which the helicase domain is shown in green and the CTD in orange. The double stranded region of the two hairpin RNA molecules used to make this model are shown in blue - with a black line representing the position of adjoining 4-base flexible regions. **(C)** The predicted scattering curve from the SASREF derived model (shown as a grey line) superposed on experimental scattering profile (shown as black spheres) of DC-RIG-I with 8bp-long in the presence of ADP-AlF$_x$. The scattering curve is shown as the log of scattering intensity [log I(s)] as a function of forward scattering vector in the units of Å^{-1}.

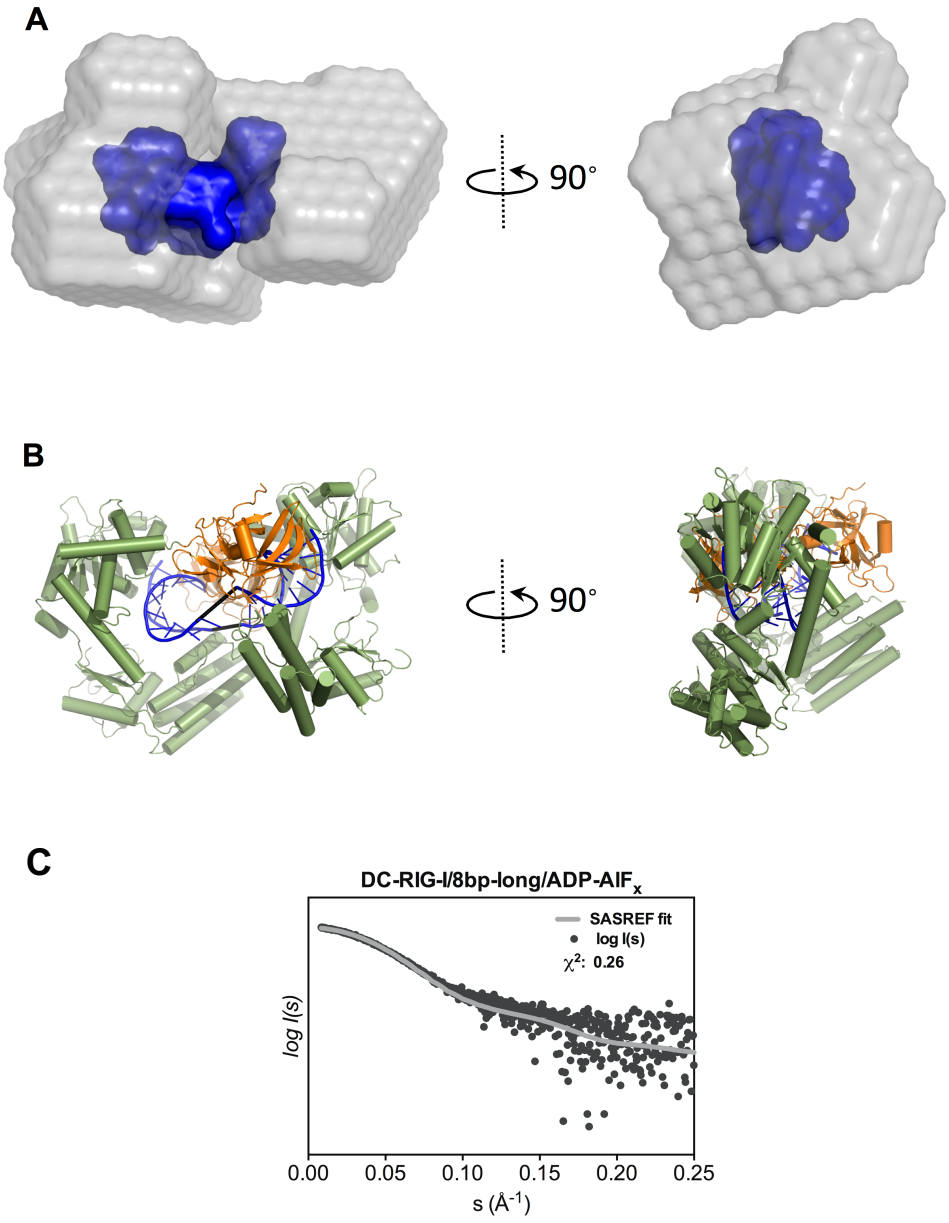

Table S1. Parameters derived from SAXS data collected for RIG-I proteins ± dsRNA ± ATP-analogues

Part A: Data collection Parameters	
Data Collection	scatterbrain IDL
Wavelength (Å)	1.03320
q range ($Å^{-1}$)	0.006-0.35
Camera length (mm)	1600
Exposure time (s)	2
Temperature	15 °C

Part B: SAXS Data and model analysis

Sample	R_g[a] (Å)	R_g[b] (Å)	R_{max} (Å)	Porod Volume ($Å^3$)	$I(0)$ guinier/ P(r)	MW[c] (kDa)	MW[d] (kDa)	DAM MIF NSD	χ^2
4AY2 (protein only)						78.7			
AMP-PNP						0.51			
ADP-AlF_x						0.53			
8bp (from 4AY2)						6.6			
10bp (created by MCSYM)						7.9			
8bp-long						13.2			
FL-RIG-I	43.4±1.4	42.2	140	186427	0.0099/ 0.0098	107.6	108.4	0.57	0.22[e]
FL-RIG-I/AMP-PNP	41.5±0.4	42.2	140	184500	0.0321/ 0.0322	108.1	108.5	0.61	
FL-RIG-I/ADP-AlF_x	41.9±1.1	43.4	156	189990	0.0510/ 0.0516	108.1	112	0.62	0.25[f]
FL-RIG-I/10bp	40.8±1.6	42.8	161	160290	0.0473/ 0.0475	115.5	94.3		0.69[f]
FL-RIG-I/10bp/AMP-PNP	42.0±1.8	43.6	170	162628	0.0484/ 0.0488	116	96		0.72[f]
FL-RIG-I/10bp/ADP-AlF_x	40.4±1.9	44.6	183	156084	0.0527/ 0.0537	116	92		0.28[f]
FL-RIG-I/8bp (peak1)	42.6±1.5	42.8	153	179388	0.0306/ 0.0307	114.2	107.8		0.50[f]

FL-RIG-I/8bp-long (peak2)	57.1±2.2	60.2	246	388547	0.0189/ 0.0193	228.4	232.8		
FL-RIG-I/8bp/AMP-PNP (peak1)	41.1±0.9	42.2	150	187731	0.0141/ 0.0141	114.7	110.4		0.59[f]
FL-RIG-I/8bp-long/AMP-PNP (peak2)	57.8±6.3	64.3	246	449575	0.0044/ 0.0046	228.9	264.4		
FL-RIG-I/8bp/ADP-AlF_x (peak1)	42.4±1.1	44.2	168	178310	0.0356/ 0.0359	114.7	104.9		0.48[f]
FL-RIG-I/8bp-long/ADP-AlF_x (peak2)	53.2±4.3	57.2	251	298493	0.0219/ 0.0222	228.9	171		
DC-RIG-I/Apo	36.7±1.6	37.8	130	113989	0.0348/ 0.0348	79.7	68.5	0.65	0.68[e]
DC-RIG-I/AMP-PNP	37.8±0.4	38.5	131	117722	0.0235/ 0.0236	80.2	71.04	0.71	
DC-RIG-I/ADP-AlF_x	35.1±1.5	36.6	140	131817	0.0457/ 0.0460	80.2	77.9	0.61	0.42[f]
DC-RIG-I/10bp	28.2±0.6	28.1	90	145960	0.0460/ 0.0459	87.6	85.06	0.51	0.52[g]
DC-RIG-I/10bp/AMP-PNP	28.2±0.7	28.2	90	134940	0.0442/ 0.0441	88.1	79.4	0.53	0.40[g]
DC-RIG-I/10bp/ADP-AlF_x	28.2±0.8	28.4	89	136914	0.0414/ 0.0414	88.1	80.1	0.54	0.57[g]
DC-RIG-I/8bp (peak1)	33.7±2.6	34.3	116	131799	0.0162/ 0.0161	86.3	77.5		0.36[f]
DC-RIG-I/8bp-long (peak2)	40.5±1.8	40.4	150	272574	0.0225/ 0.0224	172.6	160.3		
DC-RIG-I/8bp/AMP-PNP (peak1)	32.0±2.0	33.0	111	113679	0.0072/ 0.0073	86.8	66.9		0.24[f]
DC-RIG-I/8bp-long/AMP-PNP (peak2)	37.7±2.1	38.5	154	225790	0.0112/ 0.0112	173.1	132.8		
DC-RIG-I/8bp/ADP-AlF_x (peak1)	29.6±1.2	29.8	105	131925	0.0219/ 0.0219	86.8	77.6	0.57	0.27[g]
DC-RIG-I/8bp-long/ADP-AlF_x (peak2)	39.2±1.6	40.1	160	230126	0.0205/ 0.0205	173.1	135.4		0.26[h]

[a] R_g calculated from Guinier.
[b] R_g from P(r).
[c] Calculated MW (Mr) from sequence
[d] MW estimated from Porod volume using partial specific volume of 1.7
[e] χ^2 calculated using BUNCH (2)
[f] χ^2 calculated using EOM (3)
[g] χ^2 calculated using CORAL (2)
[h] χ^2 calculated using SASREF (2)

REFERNCES

1. Svergun, D.I. (1999) Restoring low resolution structure of biological macromolecules from solution scattering using simulated annealing. *Biophysical journal*, **76**, 2879-2886.
2. Petoukhov, M.V. and Svergun, D.I. (2005) Global rigid body modeling of macromolecular complexes against small-angle scattering data. *Biophysical journal*, **89**, 1237-1250.
3. Bernadó, P., Mylonas, E., Petoukhov, M.V., Blackledge, M. and Svergun, D.I. (2007) Structural Characterization of Flexible Proteins Using Small-Angle X-ray Scattering. *Journal of the American Chemical Society*, **129**, 5656-5664.